Journal of Molecular Catalysis A: Chemical 312 (2009) 40–47

Contents lists available at ScienceDirect

Journal of Molecular Catalysis A: Chemical

journal homepage: www.elsevier.com/locate/molcata

Chiral Mn (III) salen complexes covalently bonded on zirconium oligostyrenylphosphonate-phosphates as catalysts for enantioselective epoxidation of nonfunctionalized alkenes

Wenshan Ren, Xiangkai Fu*

College of Chemistry and Chemical Engineering, Southwest University, Research Institute of Applied Chemistry Southwest University, the Key Laboratory of Applied Chemistry of Chongqing Municipality, Tian Sheng Road 1, Beibei, Chongqing 400715, China

ARTICLE INFO

Article history:
Received 18 April 2009
Received in revised form 30 June 2009
Accepted 3 July 2009
Available online 10 July 2009

Keywords:
Chiral Mn (III) salen
Covalently bonded
Zirconium
oligostyrenylphosphonate-phosphates
Heterogeneous catalyst
Asymmetric epoxidation

ABSTRACT

A class of zirconium oligostyrenyl-phosphonate-phosphates in a number of stoichiometric pendant group ratios has been synthesized ($Zr(HPO_4)_{2-x}[O_3P{-}(CH(C_6H_5CH_2)CH_2)_n]_x{\cdot}mH_2O$). A general method for the covalent attachment of chiral Mn (III) salen complex to those materials has been devised. The heterogeneous catalysts showed higher chiral induction for enantioselective epoxidation of α-methylstyrene (ee, 57–71%) in the presence of pyridine N-oxide as axial base using aqueous NaOCl as oxidant than that observed in homogeneous catalyst system (ee, 54%). Meanwhile, styrene and indene were efficiently epoxidized with these supported catalysts, and the results were comparable to that for the homogeneous system. In addition, the influence of *x* values of zirconium oligostyrenyl-phosphonate-phosphates on the catalytic performance of the heterogeneous Mn (III) salen catalysts was investigated in detail. Intermediate *x* values result in intermediate steric constraints, resulting in spacing values between the two organic groups. The heterogeneous catalysts are relatively stable and can be recycled nine times.

1. Introduction

Chiral salen transition metal complexes have become a matter of current interest because of their wide applications as catalysts in several reactions [1–3] under homogeneous conditions. But homogeneous catalytic reactions always entail difficulties in separation and recycling of catalysts and purification of products, hindering practical application of homogeneous asymmetric epoxidation as well as many other homogenous reactions. Therefore, heterogenization of homogeneous catalysts has become an important strategy for obtaining supported catalysts that retain the active catalytic sites of a homogeneous analogue while at the same time providing advantages of easy separation and recycling of the catalyst [4,5]. Several papers have recently reported the heterogenization of chiral salen transition metal complexes to solid supports, including mesoporous molecular sieves [6–8], mesoporous silica [9,10] and Wangs resin [11] where the metal complexes exhibited moderate to excellent results for enantioselective epoxidation of nonfunctionalized alkenes. Furthermore, such heterogenization of chiral Mn (III) salen complex revealed that the local environment inside the mesopores and pore size of the support does affect the enantioselectivity of the epoxidation reaction [12,13]. Therefore, it is prudent to graft the active metal complex onto solid support with varied pore sizes to determine the optimum pore size for efficient diffusion of reactant and product molecules.

Zirconium phosphates and zirconium phosphonates have been extensively researched. And these materials could be used as ion-exchanger, adsorbents, ion conductivity materials and catalyst supports [14–16]. Many hybrid zirconium phosphate-phosphonates, $Zr(HPO_4)_{2-x}(O_3P{-}G)_x{\cdot}H_2O$ (*x* was varied from 0 to 2, G was the organic group in the phosphonic side chain), in which the ratios of organic groups (*x*) could be easily modulated to meet different stereo-chemistry demands were reported [17–19]. In previous work, we successfully synthesized oligostyrenyl phosphonous acid (OSPUA) using benzoyl peroxide (BPO) as initiator and explored the reaction mechanism according to mass spectral data [20]. Then zirconium oligostyrenylphosphonate-phosphate (ZSPP) and corresponding derivatives were further synthesized [21]. The frameworks of ZSPP can be easily designed and assembled to generate pores or channels of various sizes and shapes by appropriate modification of the polystyrene part. Recently, we have anchored polyamine molybdenum (VI) complexes onto chloromethyl-zirconium oligostyrenyl-phosphonate-phosphate (ZCMSPP) [22]. Meanwhile, chiral Mn (III) salen complexes axially immobilized on ZCMSPP have been explored [23,24], which performed high conversion, enantioselectivity and reusability for catalytic asymmetric epoxidation of styrene.

* Corresponding author. Tel.: +86 23 68253704; fax: +86 23 68254000.
E-mail address: fxk@swu.edu.cn (X. Fu).

1381-1169/$ – see front matter © 2009 Elsevier B.V. All rights reserved.
doi:10.1016/j.molcata.2009.07.002

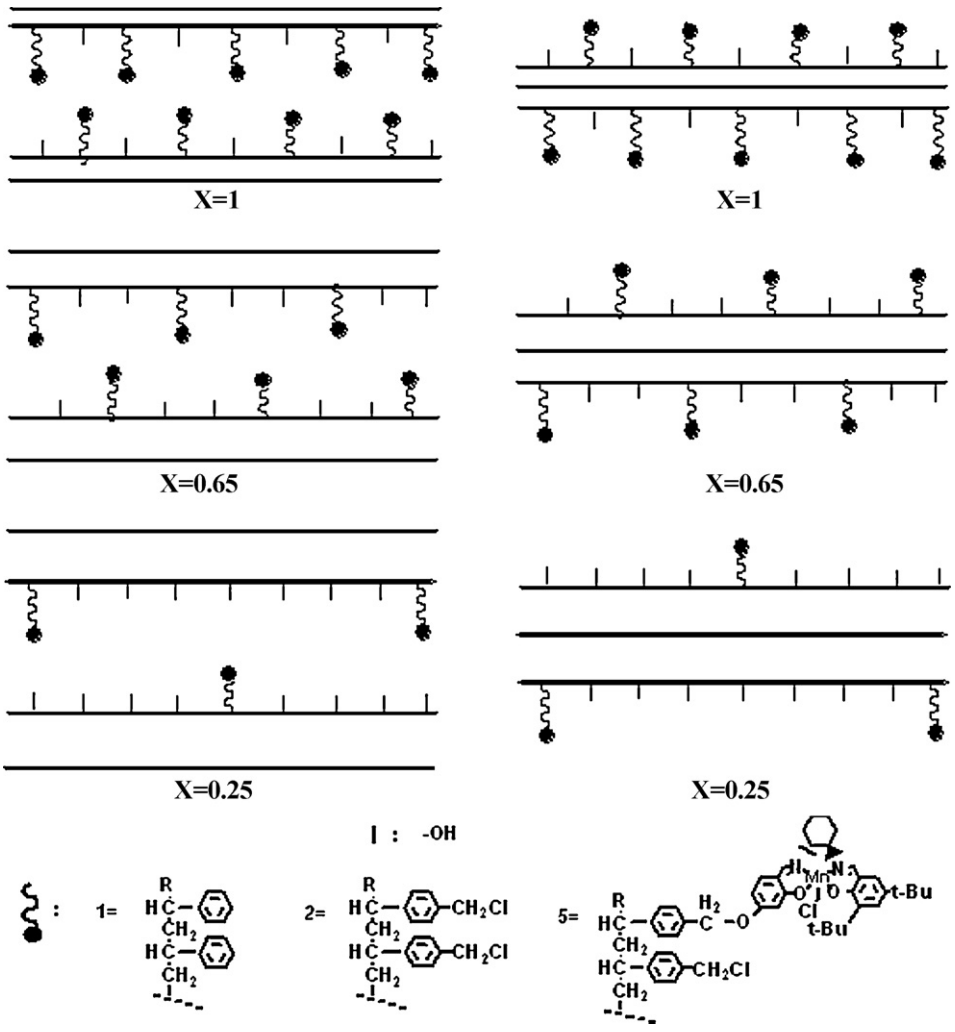

Scheme 1. Inner type (a) and outer type (b) of organic groups anchored.

Herein, a class of ZSPP in a number of stoichiometric pendant group ratios has been synthesized. Scheme 1 shows the structures of ZSPP with different *x* values. The oligostyrenyl groups are located on the external surfaces or between the layers of ZSPP. If the *x* values are big like 1a ($x = 1$) the room between two oligostyrenyl groups will be small, and in order to exclude the higher energy arrangement of pendant groups segregating on the interlayer most of the oligostyrenyl groups are pushed out and located on the external surface of ZSPP. In contrast, if *x* values are small like 1b ($x = 0.65$) and 1c ($x = 0.25$) the space between two oligostyrenyl groups will be big. And most of the oligostyrenyl groups are naturally located between the layers of ZSPP. A general method for the covalent attachment of chiral Mn (III) salen complex to those materials has been devised.

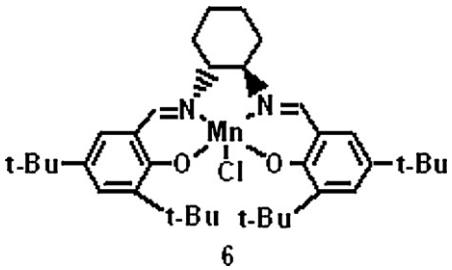

6

Scheme 2. Jacobsen's catalyst 6.

The heterogeneous chiral Mn (III) salen catalysts show comparable or even higher enantioselectivities than homogeneous chiral Mn (III) salen (Scheme 2) catalyst for the asymmetric epoxidation of various unfunctionalized olefins. The heterogeneous chiral Mn (III) salen catalyst is relatively stable and can be recycled nine times in the asymmetric epoxidation of α-methylstyrene. The excellent catalytic effect is caused by the special structures of ZSPP.

2. Experimental

2.1. Materials and instruments

(1R,2R)-(−)-1,2-Diaminocyclohexane, 2, 4-dihydroxybenzaldehyde, styrene, indene, α-methylstyrene, n-nonane, 4-phenylpyridine N-oxide (4-PPNO), N-methylmorpholine N-oxide (NMO) and m-chloroperbenzoic acid (m-CPBA) were supplied by Alfa Aesar, (1R,2R)-(−)-1,2-diaminocyclohexane monohydrochloride salt was synthesized according to the literature [25].

FT-IR spectra were recorded from KBr pellets using a Bruker RFS100/S spectrophotometer (USA), and diffuse reflectance UV–vis spectra of the solid samples were recorded in the spectrophotometer with an integrating sphere using $BaSO_4$ as standard. The Mn content of the catalysts was determined by a TAS-986G (Pgeneral, China) atomic absorption spectroscopy (AAS). ^1H NMR was determined by Bruker AV-300. X-ray photoelectron

spectroscopy (XPS) was performed on a ESCALAB250 apparatus. Scanning electron microscope (SEM) analyses were performed on KYKY-EM3200 (KYKY, China) microscopy. Transmission electron microscopy (TEM) analysis was recoded on a TECNAI10 (PHILIPS, Holand) apparatus. The BET surface areas were determined with the use of N_2 sorption data measured at 77 K (Quantachrome Autosorb-1). The sample degassed at 100 °C for 8 h before the measurements were obtained. The pore size distribution curves were obtained from a desorption isotherm using the BJH method. The conversion (with n-nonane as internal standard) and the ee values were measured by gas chromatography (GC) with Shimadzu GC2014 (Japan) instrument equipped using a chiral column (HP19091G-B213, 30 m × 30 m × 0.32 mm × 0.25 μm) and FID detector, injector 230 °C, detector 230 °C. The column temperature for styrene, indene, α-methylstyrene was in the range of 80–180 °C.

2.2. Synthesis of ZCMSPP 2

The synthesis and characterization of ZCMSPP have been reported before [21] (Scheme 3).

2.3. Synthesis of chiral salen ligand 3 [26] (Scheme 4)

A 100 ml flask was charged with (1R,2R)-(−)-1,2-diaminocyclohexane monohydrochloride salt (151 mg, 1.0 mmol), activated 4 Å molecular sieves (200 mg), and anhydrous methanol/dichloromethane (1:1, 10 ml). 2,4-Dihydroxybenzaldehyde (138 mg, 1.0 mmol) was added in one portion, the reaction mixture was stirred at room temperature for 4 h. A solution of 3,5-di-tertbutyl-2-hydroxy-benzaldehyde (234 mg, 1.0 mmol) resolved in methanol/dichloromethane (1:1, 10 ml) was added to the reaction mixture, followed by the slow addition of triethylamine (0.27 ml, 2.0 mmol). The reaction mixture was stirred for an additional 4 h followed by the removal of the solvents. The residue was dissolved in dichloromethane (20 ml), washed with water (2× 20 ml), and dried with magnesium sulfate (this product was used without further purification in the synthesis of 4 by ZCMSPP-capture). Flash chromatography of the crude product on silica gel (ether/hexanes = 1:4 to 1:1) afforded salen 1 (0.27 g, 60%) as a light yellow solid. ^{1}H NMR (300 MHz, $CDCl_3$) δ = 1.32 (s, 9 H), 1.40 (s, 9 H), 1.68 (m, 4H), 1.89 (m, 4H), 3.29 (m, 2 H), 6.33 (m, 1H), 6.63 (m, 1H), 6.87 (m, 1H), 6.98 (d, 1H), 7.34 (d, 1H),8.22 (s, 1H), 8.29 (s, 1H).

2.4. Synthesis of chiral Mn (III) salen complex 4 (Scheme 4)

Manganese inserted into the salen ligand was accomplished by adding a solution of $Mn(OAc)_2{\cdot}4H_2O$ (103.0 mg, 0.42 mmol) in 10 ml of ethanol to the salen ligand 2 (94.9 mg, 0.21 mmol) with stirring. The mixture was refluxed for 3 h under the protection of Ar. Then air was bubbled for an additional 2 h, and 26.7 mg of solid LiCl was added. After refluxing for 1 h the bead was filtered and rinsed sequentially with CH_2Cl_2, ethanol, H_2O and finally dried in vacuum to yield brown power 3.

2.5. Immobilization chiral Mn (III) salen 4 on the ZCMSPP (Scheme 5)

To a suspension of ZCMSPP (0.50 mmol Cl) that had been preswelled in 10 ml of THF for 30 min was added chiral Mn (III) salen (543 mg, 1.0 mmol), NaOH (120 mg, 3 mmol), The yellow suspension was refluxed for 24 h, then filtered and rinsed sequentially with THF, CH_2Cl_2 and finally dried in vacuum to yield the product as brown beads. The content of the manganese was determined by AAS.

2.6. Enantioselective epoxidation of nonfunctionalized alkenes

The activity of the prepared catalyst was tested for the epoxidation of styrene (1.0 mmol), indene (1.0 mmol), α-methylstyrene (1.0 mmol) in CH_2Cl_2 (2 ml) containing n-nonane (internal stan-

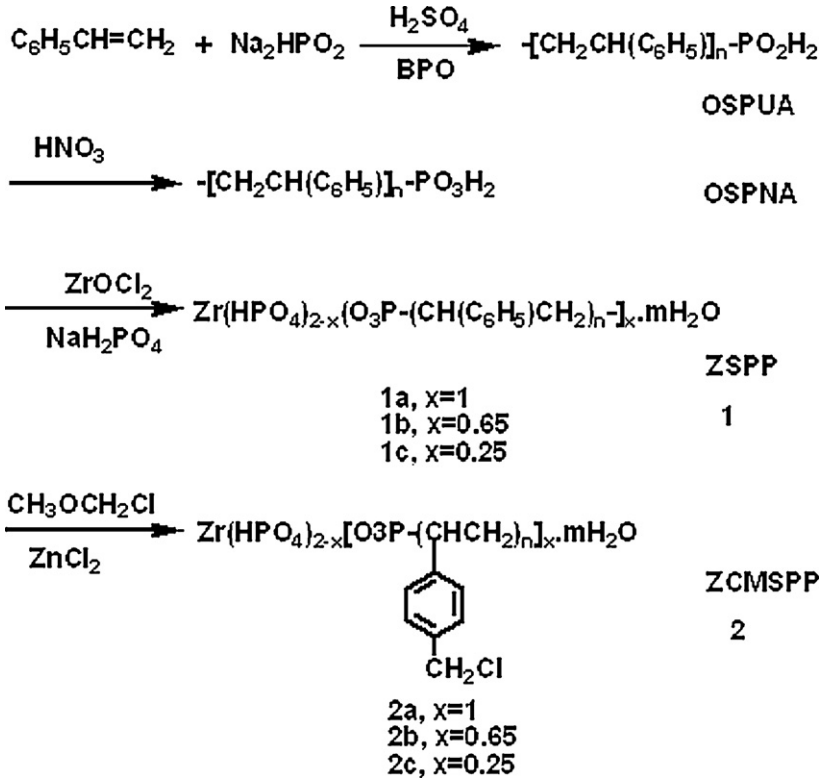

Scheme 3. Synthesis of the supports.

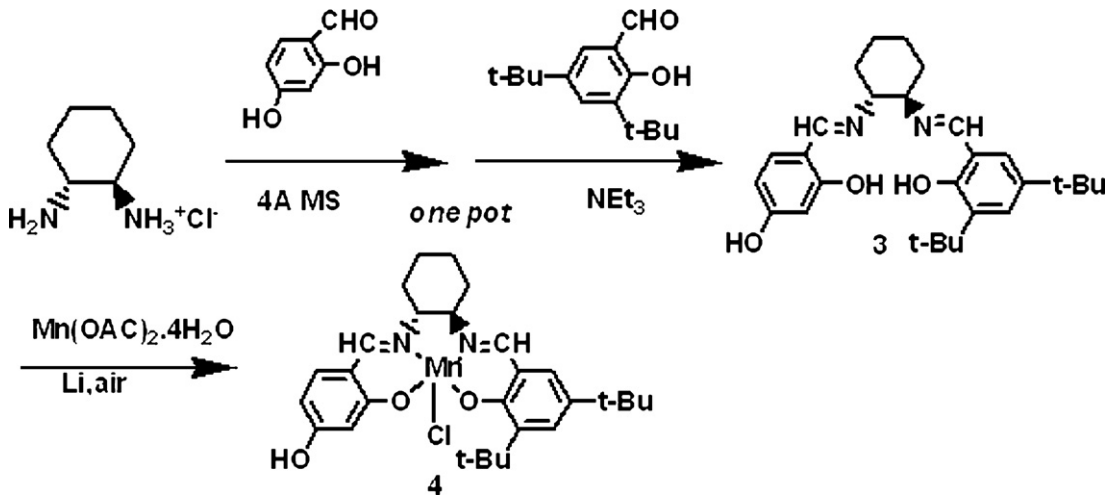

Scheme 4. Synthesis of the chiral Mn (III) salen.

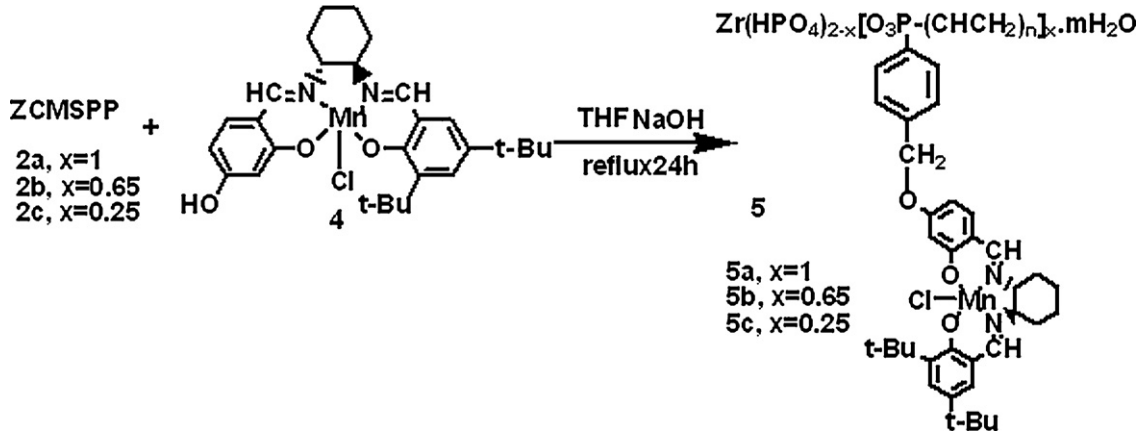

Scheme 5. Immobilization chiral Mn (III) salen on ZCMSPP.

dard), 4-PPNO (0.38 mmol), NaClO (pH 11.35, 0.55 M, 3.6 ml) and the catalysts (5 mol%). The conversion and ee values of the epoxides were determined by GC.

2.7. The reusability of the catalyst

In a typical recycle experiment, the equal volume of hexane was added to the reaction mixture after the reactions, then the organic phase was separated, and the used black catalyst was washed with hexane and water, and then dried over vacuum at 60 °C to remove the remaining hexane and water. The recovered dried solid catalyst was weighed and reused in the next run. In every run the same ratio of the substrate-to-catalyst and solvent-to-catalyst was kept.

3. Results and discussion

3.1. Spectral analysis

IR spectra of the support ZCMSPP and heterogeneous chiral Mn (III) salen catalysts were recorded in the range of 4000–400 cm^{-1} (Fig. 1).

The spectra of ZCMSPP (Fig. 1) show the typical intense and broad bands centered at 1030 cm^{-1}, which are attributed to the P–O stretching vibration in the support ZCMSPP. The –O–H stretching vibration extended from 3000 to 3500 cm^{-1} is assigned to the hydrogen bond of hydroxyl group and H_2O. The sharp absorption bands at 1600–1450 are attributed to the characteristic absorption of phenyl group of the supports. The IR bonds at 2935, 1405, 1365 cm^{-1} are assigned to C–H vibration of alkyl groups.

Upon bonding of chiral Mn (III) salen onto ZCMSPP (Fig. 1d–f), several changes in the FT-IR spectrum can be observed in all the frequency range. The stretching vibration at 1030 cm^{-1} which is assigned to characteristic vibrations of the phosphonic acid group in ZSPP becomes weak due to the structure changes for the host–guest interaction [21]. The additional peaks at 1125, 1229 and 1258 cm^{-1}

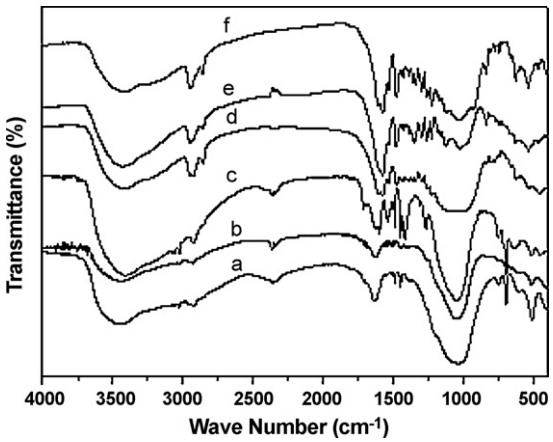

Fig. 1. FT-IR spectra of (a) 2a, (b) 2b, (c) 2c, (d) 5a, (e) 5b, (f) 5c.

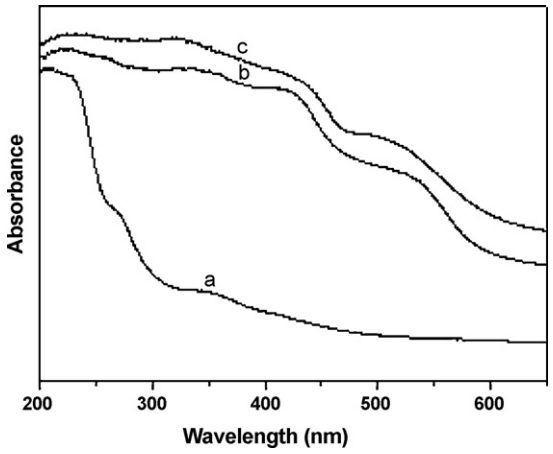

Fig. 2. UV–vis spectra of (a)2b, (b) 5b, (c) 6.

demonstrate the formation of the ether link between chiral Mn (III) salen and ZSPP, and the intensity increase of C–H vibration of alkyl groups at 2935 and 2863 also suggests that the homogeneous chiral Mn (III) salen catalyst is immobilized to ZSPP. Furthermore the new bond around 1608 cm^{-1} is the characteristic vibrations of C=N stretching of chiral Mn (III) salen.

Diffuse reflectance UV–vis spectra (Fig. 2) also give obvious evidence for the successful immobilization. The ZCMSPP 2b presents only the bond of phenyl groups of 200–300 nm in UV–vis spectra (Fig. 2a). Homogeneous chiral Mn (III) salen (Fig. 2c) and the supported chiral catalyst (Fig. 2b) show similar bands at 253, 430 and 500 nm in UV–vis spectra. The bands at 253 nm may be assigned to the π–π^* transition of the phenyl groups. The peaks at 430 and 500 nm are the characteristic bonds of the chiral Mn (III) salen system [13].

XPS (Fig. 3) spectrum gives further evidence for the successful immobilization based on the fact that the characteristic bond at 642 eV of $Mn2P_{3/2}$ is clear.

3.2. Surface morphology and structures of the catalysts

SEM was used as a tool to understand the surface morphology of the catalysts. The figure shows that surface morphology of the catalyst is loose and amorphous. TEM clearly shows that there are many micopores and secondary channels among the layers of the catalyst (Fig. 4b). These micopores and secondary channels will increase the surface area of the catalysts [22] and provide enough space for substrates to access to the catalytic active sites. According to the surface morphology, the ideal model of immobilized catalysts 5 was deduced in Fig. 5 [23].

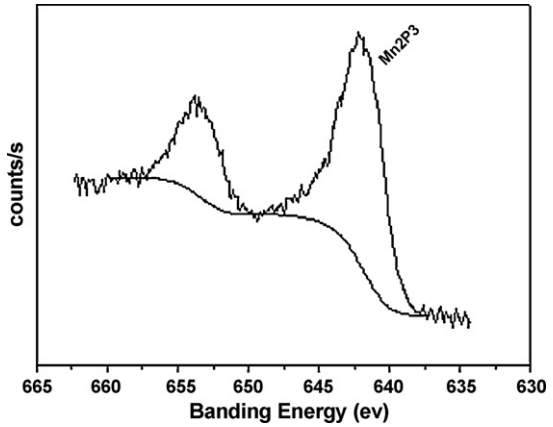

Fig. 3. XPS spectrum of 5b.

3.3. Enantioselective epoxidation of nonfunctionalized alkenes

The catalytic activity of immobilized catalysts for the epoxidation of styrene, α-methylstyrene and indene was studied in CH_2Cl_2 with NaClO as oxidative system. Jacobsen's catalyst 6 (Scheme 2) was also examined for comparison purposes. The data obtained are summarized in Table 1. The supported chiral catalysts exhibit comparable or even higher enantioselectivities than homogeneous chiral Mn (III) salen catalyst 6 for the asymmetric epoxidation of some unfunctionalized olefins.

Table 1 shows the results of the asymmetric epoxidation of styrene catalyzed by homogeneous and heterogeneous chiral Mn (III) salen catalysts. Homogeneous chiral Mn (III) salen 6 gives an ee value of 38% (entry 1). The immobilized chiral Mn (III) salen catalyst 5b ($x = 0.65$) shows ee value comparable to that of the homogeneous catalyst (entry 4). While, under the same conditions, the immobilized chiral Mn (III) salen catalyst 5a ($x = 1.00$) shows ee value of 28% (entry 5), lower than the ee value of 34% for the catalyst immobilized in 1b. A possible explanation may be that the content and the concentration of the organic parts for 2a are much higher than those of 2b and 2c (Scheme 1), thus space between two organic groups is very small. The evidence is the nitrogen sorption (BET) results of ZCMSPP in Table 2. 2a has smaller nanopore size (around 1.3 nm) and pore volume (0.15 cm^3/g) than 2b (nanopore size around 3.2 nm and pore volume 0.50 cm^3/g) and 2c (nanopore size around 4.0 nm and pore volume 0.64 cm^3/g), and the solvated chiral Mn (III) salen complex 4 is around 1.6 nm which is too large to be accommodated into the nanopores of 2a [27]. Therefore, most of the chiral Mn (III) salen complex is immobilized onto the external surface of 2a (Scheme 1). Therefore, 2a cannot afford confinement effect originated from the nanopores which enhances chiral recognition between the immobilized chiral Mn (III) salen catalyst and the substrate [27]. In contrast, when catalyst is supported between the layers of the materials like 2b and 2c the enantioselectivity will

Table 1
Catalytic performance of the catalysts for enantioselective epoxidation of alkenes.

Entry	Substrate	Catalyst	Time (h)	T (°C)	Yield (EO)[a] (%)	ee (%)
1	Styrene	6	5	0	>99.0	38.5[b]
2		5b	5	0	40.7	32 .3[b]
3		5b	8	0	45.9	31.9 [b]
4		5b	12	0	51.4	34.7[b]
5		5a	12	0	50.9	27.8[b]
6		5c	12	0	54.3	31.2[b]
7	α-Methylstyrene	6	6	20	>99.0	54.0[c]
8		5b	12	20	40.1	63.2[c]
9		5b	24	20	45.5	65.7[c]
10		5b	24	0	30.0	70.8[c]
11		5a	12	20	73.6	51.7[c]
12		5c	12	20	50.8	57.5[c]
13	Indene	6	6	0	92	65[d]
14		5b	24	0	20.9	33.4[d]
15		5a	24	0	60.0	38 .1[d]
16		5c	24	0	66.4	63.2[d]

[a] Reactions were performed in CH_2Cl_2 (2 mL) with styrene (1.0 mmol), indene (1.0 mmol), α-methylstyrene (1.0 mmol), n-nonane (internal standard), 4-PPNO (0.38 mmol), homogeneous (3 mol%) or heterogeneous chiral Mn (III) salen catalysts (3 mol%) and NaClO (pH 11.35, 0.55 M, 3.6 ml). The yield and the ee values were determined by GC with chiral capillary columns HP19 091G-B213, 30 m × 0.32 mm × 0.25 μm. EO: epoxide.

[b] Expoxide configuration S.

[c] Epoxide configuration S.

[d] Epoxide configuration 1S, 2R.

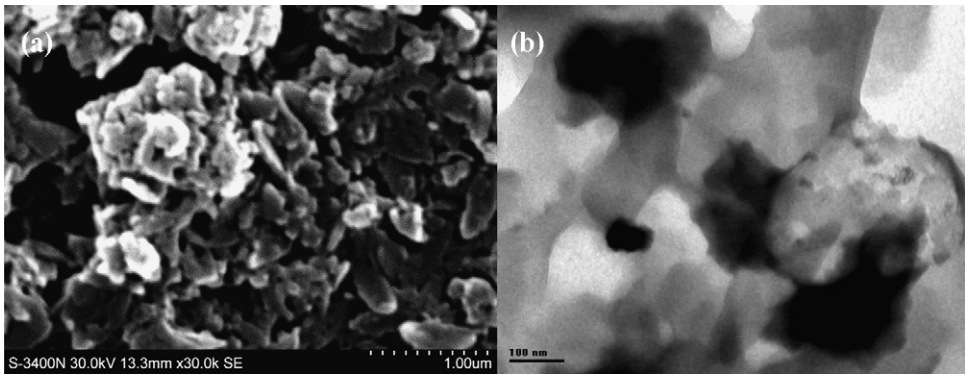

Fig. 4. The SEM photograph of (a) 5b and TEM photograph of catalyst (b) 5b.

be enhanced, and Caplan et al. also found the confinement effect for the asymmetric epoxidition of styrene [28].

α-Methylstyrene was then chosen to investigate the heterogeneous chiral Mn (III) salen catalysts. It is interesting to note that the heterogeneous chiral Mn (III) salen catalysts in NaClO oxidative system display excellent enantioselectivity (Table 1). The ee values (57–71%) with the catalysts of 5b and 5c are higher as compared with Jacobsen's catalyst 6 (ee, 54%). Similar results were obtained by Kim and Shin [29] and Xiang et al. [30]. Kim and Shin reported that, for the asymmetric epoxidation of α-methylstyrene, the ee increased from 51 to 59% after immobilization of chiral Mn (III) salen on the siliceous MCM-41 by multi-step grafting. The increase in enantiomeric excess may also be attributed to the microenvironment effect and confinement effect differing from either pure polystyrene or inorganic supports [23], these effects are provided by the layered structure and micropores of ZSPP and the balance adjustment between the hydrophobic of polystyrene parts and the hydrophilic of phosphate parts. And these features are different from either pure polystyrene or pure zirconium phosphates. However, 5a exhibits lower ee value (52%) than homogeneous chiral Mn (III) salen catalyst 6 (54%). The reason is also as mentioned above. Moreover, the ee values increase slightly with decreasing temperature (entries 9 and 10).

These heterogeneous chiral Mn (III) salen catalysts were also tested for the asymmetric epoxidation of the relatively bulkier alkene like indene (entries 13–16). These reaction results show that the enantioselectivity and activity of the immobilized catalyst 5b for indene (ee, 33% yield 21%) (entry 14) are found to be lower than that of 5c (entry 16) and neat homogenous 6 (ee, 92% yield 65%) (entry 13), the reason may be that indene is too large to accommodate into the micropores and layers of ZSPP. Therefore, indene may merely react with a few active sites on the external surface of the ZSPP and 5b cannot afford confinement effect for indene. Meanwhile, under the same conditions the yield of the epoxide with 5a (entry 15) are better than those of 5b (entry 14), but they show comparable ee values. One possible explanation for this result is that the amount of chiral salen Mn (III) catalytic active centers on external surface for 5a is much more than that for 5b.

Table 2
The results of N_2 adsorption of supports[a].

Entry	Sample (x)	Pore size[b] (nm)	S_{BET}[c] (m^2/g)	Pore volume[d] (cm^3/g)
1	1	1.3	34	0.15
2	0.65	3.2	66	0.50
3	0.25	4.0	73	0.64

[a] The sample were degassed at 100 °C for 8 h.
[b] Pore size based on the desorption data using BJH method.
[c] Surface based on multipoint BET method.
[d] Pore volume based on the desorption data of BJH method.

So the enantioselectivity in the asymmetric catalytic reactions is usually decreased for the immobilized chiral catalysts compared to homogeneous counterparts. However, in many cases, the catalysts confined in nanopores show comparable or even higher ee values than the homogeneous catalysts, which are simply attributed to the confinement effect of the nanopores [31]. However, the detailed insights of the confinement effect were not well understood.

Table 1 also gives the tendency of changing yields. Generally, the yields of products are lower for the heterogeneous chiral Mn (III) salen catalysts than those for the homogeneous catalysts, due to the difficulty in diffusion. As for the asymmetric epoxidation of styrene, three of the heterogeneous chiral Mn (III) salen catalysts 5a, 5b and 5c get the comparable yields. However, for the bulkier olefins like α-methylstyrene and indene the heterogeneous chiral Mn (III) salen catalyst with small x value as 5c ($x = 0.25$) can obviously have better yields than that of with big x value as 5b ($x = 0.65$). With decreasing of the ratio of the organic groups the space of two neighboring chiral salen Mn (III) catalytic active centers (Scheme 1a) will increase, thus 5c ($x = 0.25$) has the bigger room than that of 5b ($x = 0.65$) for the diffusion of bulkier olefins.

3.4. The x values of ZSPP on confinement effect

The results of the enantioselective epoxidation of nonfunctionalized alkenes exhibit the effect of the x value (ZSPP) on the confinement effect of the heterogeneous chiral Mn (III) salen catalysts.

ZSPP can be formed by coprecipitation of the zirconium in the presence of oligostyrenylphosphonic acid (P–G) and phosphoric acid (P–OH), leading to the formation of a porous hybrid mate-

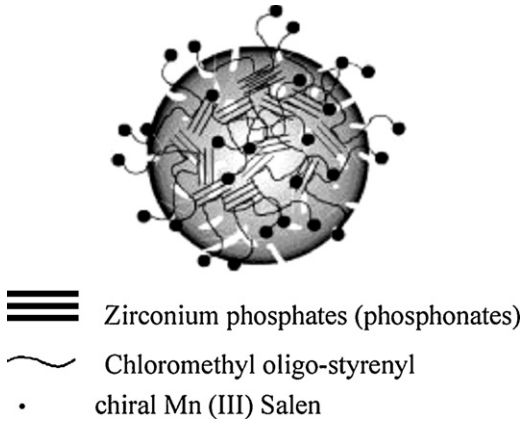

Fig. 5. Deduced models of the supported chiral Mn (III) salen catalysts 5. (≡) zirconium phosphates (phosphonates), (∼) chloromethyl oligostyrenyl, (●) chiral Mn (III) salen.

rial because the groups of P–G and P–OH are sufficiently different in size. These hybrid compounds usually contain a random distribution of the organic groups such that all layers have identical stoichiometry. In such systems, the interlayer spacing (*d*-space) is a function of pendant group stoichiometry, and has a generally linear dependence on component mole fraction [32]. Intermediate *x* values result in intermediate steric constraints, resulting in *d* values between the two organic groups.

Then the models of $Zr(HPO_4)_{2-x}[O_3P{-}(CH(C_6H_5)CH_2)_n]_x{\cdot}mH_2O$ series, viz. where $x = 1.0, 0.65, 0.25$ were deduced. As we know, each zirconium atom is bonded to six oxygen atoms, and every three of these oxygen atoms are bonded to one phosphorus atom. As a result, the layers of the ZSPP are formed. A layer of the 1a ($x = 1$) presents that in order to exclude the higher energy arrangement of pendant groups segregating on the interlayer, there is always a P–G (B) groups insert between two P–OH (A) or reverse. That is to say, the ideal model can be simply denoted as "ABABAB. . .". And the scheme of the ideal cross-section (Fig. 6) indicates that two P–G (B) and four P–OH (A) groups are located around one P–G group, sterically directed energy allows P–G groups to get out of the layers.

Similarly, the ideal model for 1b ($x = 0.65$) can also be denoted as "AABAABAAB. . .". And the scheme of the ideal cross-section (Fig. 6) suggests that six p–G (B) groups are located around one p–G group (some big p–G groups may also get out of the layers). The *d*-space is bigger than that of 1a, and it can offer enough space for some smaller substrates coordination to the active sites. Meanwhile, confinement effect generated for steric hindrance among the substrates and active sites.

For 1c ($x = 0.25$) the ideal model can also be denoted as "BAAAAAAABAAAAAAABAA. . .", and the scheme of the ideal cross-section (Fig. 6) suggests that the space of two neighboring P–G groups is much larger than 1b and 1c. Although there is big room for catalytic reaction, the confinement effect and the content of the active sites always are decreased.

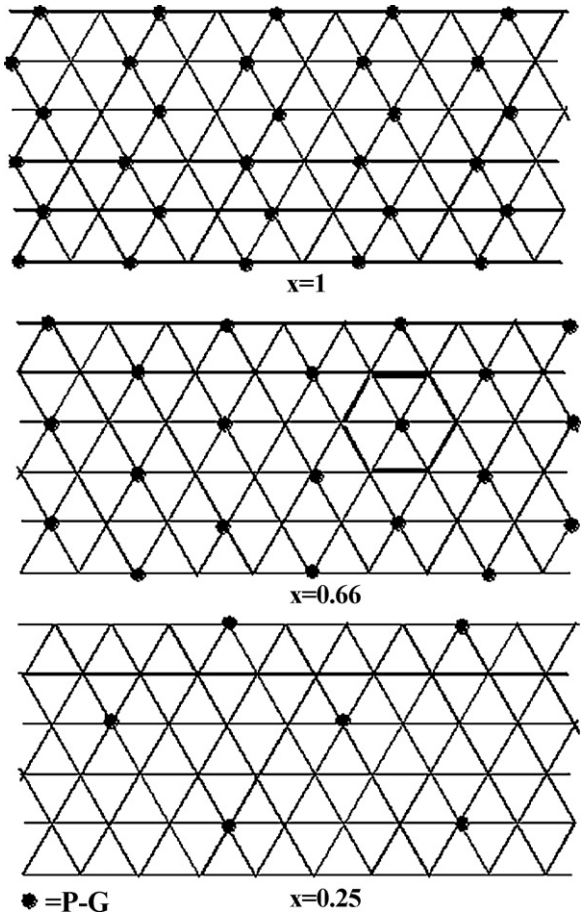

Fig. 6. The cross-section of the 1a ($x = 1$), 1b ($x = 0.65$) and 1c ($x = 0.25$).

Table 3
Recycle of catalyst 5b ($x = 0.65$) in asymmetric epoxidation of α-methylstyrene.

Entry	Yield (%)	ee [a,b] (%)
1	45.5	65.7
2	38.4	68.2
3	33.3	64.5
4	30.5	67.3
5	28.8	64.9
6	26.4	63.1
7	23.0	60.5
8	20.1	61.0
9	14.8	57.4

[a] The reaction conditions are the same as in Table 1 of entry 9.
[b] Epoxide configuration S.

Qualitatively, the changes in the *d*-spacing with composition can be rationalized in terms of interrelated factors that pertain to the steric interactions of the bulkier oligostyrenyl groups and the conformations of the organic groups.

3.5. The reusability of the catalyst

The reuse of the heterogeneous chiral Mn (III) salen catalysts 5b ($x = 0.65$) was one of the most valuable and attractive properties. In the reaction process the particles of heterogeneous chiral Mn (III) salen catalysts were suspended in the reaction mixture of the epoxidation of alkenes. After reactions the product could be separated by adding the same volume of hexane, and the catalyst would precipitate from the remainder solution. Above 95% recycle of the catalyst was achieved in every run. The recovered dried solid catalyst was weighed and reused in the next run. In every run the same ratio of the substrate-to-catalyst and solvent-to-catalyst was kept.

After being recycled nine times there was little decrease in enantioselectivity, even though the yield decreased sharply from about 46 to 15% (Table 3). The reason for good stability of the heterogeneous chiral Mn (III) salen catalyst may be the effective separation the chiral Mn (III) salen complexes by the solid support ZSPP so that they cannot dimerize to inactive μ-oxo-Mn(IV) species [33]. The decrease of the yield can be due to the decomposition of the chiral Mn (III) salen complex under epoxidation conditions [34] and the loss of the hyperfine granules of the heterogeneous chiral Mn (III) salen catalysts (formed in reaction due to stirring). The Mn content of the heterogeneous catalyst 5b is 0.42 mmol/g compared with the total amount (around 0.66 mmol/g) when the heterogeneous catalyst reused for nine times. The decomposition of the Mn (III) salen complex under epoxidation conditions was also noted by Aggelino et al. and Song et al. [34,35]. Meanwhile, micropores and secondary channels were partly plugged after several recycle epoxidations [23].

4. Conclusions

ZCMSPP with the different content of the organic group (*x*) were synthesized. Chiral Mn (III) salen complexes were supported onto these materials by a covalent grafting method. The structures of the heterogeneous chiral Mn (III) salen catalysts were characterized by IR, diffuse reflectance UV–vis, XPS, and the surface morphology of the catalysts recorded with SEM was discussed. The supported chiral Mn (III) salen catalyst exhibits comparable or even higher enantioselectivities than that of homogeneous catalyst for the asymmetric epoxidation of several unfunctionalized olefins in

the presence of NaClO. In addition, the influence of *x* values on the catalytic performance of the heterogeneous Mn (III) salen catalysts was investigated in detail. The heterogeneous chiral Mn (III) salen catalysts are relatively stable and can be recycled nine times in the asymmetric epoxidation of α-methylstyrene. The excellent performances of the hetrogeneous catalysts are attributed to the special structure of ZSPP.

Acknowledgement

Authors are grateful to Southwest University of China for the financial support.

References

[1] P. Piaggio, P. McMorn, D. Murphy, D. Bethell, P.C. Bulman Page, F.E. Hancock, C. Sly, O.J. Kerton, G.J. Hutchings, J. Chem. Soc., Perkin Trans. 2 (2000) 2008–2015.
[2] T. Niimi, T. Uchida, R. Irie, T. Katsuki, Tetrahedron Lett. 41 (2000) 3647–3651.
[3] V. Ayala, A. Corma, M. Iglesias, J.A. Rinĭcon, F. Sánchez, J. Catal. 224 (2004) 170–177.
[4] P. Smet, J. Riondato, T. Pauwels, L. Moens, L. Verdonck, Inorg. Chem. Commun. 3 (2000) 557–562.
[5] S. Aerts, H. Weyten, A. Buekenhoudt, L.E.M. Gevers, I.F.J. Vankelcom, P.A. Jacobs, Chem. Commun. (2004) 710–711.
[6] X. Zhou, X. Yu, J. Huang, S. Li, L. Li, C. Che, Chem. Commun. (1999) 1789–1790.
[7] L. Saikia, D. Srinivas, P. Ratnasamy, Micropor. Mesopor. Mater. 104 (2007) 225–235.
[8] S. Xiang, Y. Zhang, Q. Xin, C. Li, Chem. Commun. (2002) 2696–2697.
[9] B.M. Choudary, M.L. Kantam, B. Bharathi, P. Sreekanth, F. Figueras, J. Mol. Catal. A 159 (2000) 417–421.
[10] C. Baleizao, B. Gigante, H. Garcia, A. Corma, J. Catal. 215 (2003) 199–207.
[11] C. Borriello, R.D. Litto, A. Panunzi, F. Ruffo, Inorg. Chem. Commun. 8 (2005) 717–721.
[12] S. Xiang, Y. Zhang, Q. Xin, C. Li, J. Chem. Soc., Chem. Commun. (2002) 2696–2697.
[13] F. Bigi, L. Moroni, R. Maggi, G. Sartori, J. Chem. Soc., Chem. Commun. (2002) 716–717.
[14] A. Clearfield, D.S. Thakur, Appl. Catal. 26 (1986) 1–26.
[15] R.Q. Zeng, X.K. Fu, C.B. Gong, Y. Sui, J. Mater. Sci. 41 (2006) 4771–4776.
[16] S. Nakayama, K. Itoh, J. Eur. Ceram. Soc. 23 (2003) 1047–1052.
[17] C.Y. Yang, A. Clearfield, React. Polym. Ion Exchange Sorbents 5 (1987) 13–21.
[18] X.B. Ma, X.K. Fu, J. Mol. Catal. A: Chem. 208 (2004) 129–133.
[19] R.Q. Zeng, X.K. Fu, J. Mol. Catal. A: Chem. 209 (2005) 1–5.
[20] Y. Sui, X.K. Fu, X.B. Ma, J.R. Chen, R.Q. Zeng, React. Funct. Polym. 64 (2005) 55–62.
[21] Y. Sui, X.K. Fu, J.R. Chen, X.B. Ma, R.Q. Zeng, Mater. Lett. 59 (2005) 2115–2119.
[22] Y. Sui, X.N. Fang, R.H. Hu, Y.P. Xu, X.C. Zhou, X.K. Fu, Mater. Lett. 61 (2007) 1354–1357.
[23] R.F. Bai, X.K. Fu, H.B. Bao, W.S. Ren, Catal. Commun. 9 (2008) 1588–1594.
[24] H.B. Bao, X.K. Fu, R.F. Bai, W.S. Ren, X.B. Tu, Chem. J. Chin. Univ. 29 (2008) 927–931.
[25] E.J. Campbell, S.B.T. Nguyen, Tetrahedron Lett. 42 (2001) 1221–1225.
[26] M. Holbach, X.L. Zheng, C. Burd, C.W. Jones, M. Weck, J. Org. Chem. 71 (2006) 2903–2906.
[27] H. Zhang, Y. Zhang, C. Li, J. Catal. 238 (2006) 369–381.
[28] N.A. Caplan, F.E. Hancock, P.P.C. Bulman, G.J. Hutchings, Angew. Chem. Int. Ed. 43 (2004) 1685–1688.
[29] G.J. Kim, J.H. Shin, Tetrahedron Lett. 40 (1999) 6827–6830.
[30] S. Xiang, Y.L. Zhang, Q. Xin, C. Li, Chem. Commun. (2002) 2696–2697.
[31] C. Li, H.D. Zhang, D.M. Jiang, Q.H. Yang, Chem. Commun. (2007) 547–558.
[32] J.C. Amicangelo, W.R. Leenstra, J. Am. Chem. Soc. 120 (1998) 6181–6182.
[33] C. Li, Catal. Rev. Sci. Eng. 46 (2004) 419–492.
[34] C.E. Song, E.J. Roh, B.M. Yu, D.Y. Chi, S.C. Kim, K.J. Lee, Chem. Commun. (2000) 615–616.
[35] M.D. Aggelino, P.E. Laibinis, J. Polym. Sci. Part A: Polym. Chem. 37 (1999) 3888–3898.